Rapporto n° 202

The Autodependogram:

A Graphical Device to Investigate Serial Dependences

Luca Bagnato, Antonio Punzo, Orietta Nicolis

Dicembre 2010

Dipartimento di Metodi Quantitativi per le Scienze Economiche ed Aziendali
Università degli Studi di Milano Bicocca
Via Bicocca degli Arcimboldi 8 - 20126 Milano - Italia
Tel +39/02/64483102/3 - Fax +39/2/64483105
Segreteria di redazione: Andrea Bertolini

The Autodependogram: A Graphical Device to Investigate Serial Dependences

Luca Bagnato[*] Antonio Punzo[†] Orietta Nicolis[‡]

Abstract

In this paper the serial dependences between the observed time series and the lagged series, taken into account one-by-one, are graphically analyzed by what we have chosen to call the "autodependogram". This tool, is a sort of natural nonlinear counterpart of the well-known autocorrelogram used in the linear context. The simple idea, instead of using autocorrelations at varying time lags, exploits the χ^2-test statistics applied to convenient contingency tables. The usefulness of this graphical device is confirmed by simulations from certain classes of well-known models, characterized by randomness and also by different kinds of linear and nonlinear dependences. The autodependogram is also applied to both environmental and economic real data. In this way its ability to detect nonlinear features is highlighted.

Key words: Nonlinear time series, Serial dependences, χ^2-test, Autocorrelogram.

1 Introduction

In modelizing observed time series, the most popular approach consists in adopting the class of linear models. In this wide class, the well-known *white noise* process – characterized only by the properties of its first two moments – represents the building block and reflects information that is not directly observable. Nevertheless, the limitations of linear models already appear in the classical paper by Moran (1953). Nowadays, we know that there are nonstandard features,

[*]Dipartimento di Metodi Quantitativi per le Scienze Economiche e Aziendali - Università di Milano-Bicocca (Italy), e.mail: luca.bagnato@unimib.it

[†]Dipartimento Impresa, Culture e Società - Università di Catania (Italy), e.mail: antonio.punzo@unict.it

[‡]Dipartimento di Ingegneria dell'Informazione e Metodi Matematici - Università di Bergamo (Italy), e.mail: orietta.nicolis@unibg.it

commonly referred to as *nonlinear features* (Jianqing and Qiwei, 2003) that, by definition, cannot be captured in the linear frame. In the attempt to overcome this problem, nonlinear models have to be taken into account (for a discussion on the chief objectives which guarantee the introduction of nonlinear models, see for example, Tjøstheim, 1994). For these kinds of models, as indicated by Jianqing and Qiwei (2003), a white noise process is no longer a pertinent building block as we have to look for measures beyond the second moments to characterize the nonlinear dependence structure. Thus, the white noise has to be replaced by a noise process composed of independent and identically distributed (*i.i.d.*) variables.

As for serial correlation (better known as *autocorrelation*) in the linear case, the analysis of serial dependence (that for analogy, could be defined as *autodependence*) is then fundamental in the nonlinear approach. The term "serial" emphasizes that the dependence/correlation structure is analyzed as a function of the time lags. Studying the serial dependence of a time series, besides being useful *per se*, could be motivated by at least two other reasons. First, it is often a preliminary step carried out before modeling the data generating process (*model selection*); for example, it is common practice in finance to check serial dependence on increments of log prices or exchange rates (Bera and Robinson, 1989; Booth Teppo and Yli-Olli, 1994; Lo, 2000). Second, it can be a final step, once a nonlinear model is fitted to the observed data, to check possible serial dependences among estimated residuals (*model validation*; see, *e.g.*, Diks and Panchenko 2007 who investigate the behavior of their test of serial independence when applied to estimated residuals).

The first step in an attempt to investigate the serial dependence structure consists in adopting a test specifically conceived for it. In these terms, the statistical literature with particular reference to the nonparametric one, contains a large number of serial independence tests, the most famous of which is undoubtedly the BDS test of Brock *et al.* (1996). The interested reader is referred to Diks (2009) for a recent and detailed survey of all these methods (see also Dufour *et al.* 1982 and Hallin and Puri 1992). Nevertheless, a difference between the study of serial correlatedness and serial dependence remains. While in the former case a preliminary explorative investigation can be provided by the use of the autocorrelogram, in the latter case we do not have an analogous of this graphical device. To the best of the authors' knowledge, the only attempts in these terms are the proposals by Genest and Rémillard (2004) and Bagnato and Punzo (2010) that suggest two diagrams, called respectively dependogram and lag subsets dependence plot, allowing for a visual inspection of the subsets of lags leading to a possible rejection of the null hypotheses in account. However, these graphical devices besides being different in principle to the classical autocorrelogram, are also less simple to use.

In this paper we propose a graphical representation called autodependogram, that can be really considered as the analogous of the autocorrelagram when the dependence structure to be analyzed is the distributive one. The proposal takes advantage of the well-known χ^2-test applied to pairs of lagged variables. Obviously, being based on the χ^2-test, the proposal is valid asymptotically and it can also be applied in presence of missing data.

Proposal and paper can be so schematically summarized: Section 2 begins by presenting the common setting for both autocorrelogram and autodependogram. Although treatment is carried out directly on the observed data, it can also be easily extended in the model validation phase to the estimated residuals from a linear/nonlinear model. Section 3 describes the proposal in detail, while Section 3.1 puts forward a simple way to select the unknown quantities characterizing the autodependogram. Its behavior, in comparison with the autocorrelogram, is shown in all simulations and applications reported in Section 4 and Section 5. More specifically, in Section 4.1 two simple examples are provided using well-known models in time series literature. In Section 4.2 the performance of the autodependogram, in terms of size and power of each of its bar, is evaluated by simulations for a wide range of serial dependence alternatives. Section 5 presents two applications respectively related to ozone concentrations and natural gas prices. Finally, in Section 6, conclusive remarks, but also a brief discussion, are given.

2 Some preliminary notes: the autocorrelogram

Let $\{X_t\}_{t\in\mathbb{N}}$ represent a strictly stationary stochastic process. Moreover, let $\{x_1,\ldots,x_n\}$ be an observed time series, of length n, from $\{X_t\}_{t\in\mathbb{N}}$, where n denotes the last temporal instant. Choosing a positive integer r representing the lag, with $r<n$, it is possible to obtain the rth delayed observed series $\{x_1,\ldots,x_{n-r}\}$.

Now, suppose that we are interested in (graphically) studying the serial dependences of $\{X_t\}_{t\in\mathbb{N}}$, as a function of r, using the observed counterpart $\{x_1,\ldots,x_n\}$. The first kind of serial dependence structure that comes to mind to study, is without doubt, the linear one. To do this, the well-known autocorrelation function (ACF) is commonly considered; it describes the autocorrelations between X_t and its lag X_{t-r} as a function of r. In this case, the less restrictive weak stationarity can be assumed.

The graphical representation of an ACF is often referred to as autocorrelogram. In order to define this, we ideally construct a scheme, as in Table 1, in which l represents the maximum value chosen for r. Thus, the sample autocorrelations

$$\widehat{\rho}_r = \frac{\frac{1}{n}\sum_{t=r+1}^{n}(x_t-\bar{x})(x_{t-r}-\bar{x})}{\frac{1}{n}\sum_{t=1}^{n}(x_t-\bar{x})^2}, \quad r=1,\ldots,l, \tag{1}$$

Table 1: *Preliminary scheme to compute autocorrelations.*

X_t	X_{t-1}	X_{t-2}	$\cdots$	X_{t-r}	$\cdots$	X_{t-l}
x_1						
x_2	x_1					
x_3	x_2	x_1				
$\vdots$	$\vdots$	$\vdots$	$\ddots$			
x_{r+1}	x_r	x_{r-1}	$\cdots$	x_1		
$\vdots$	$\vdots$	$\vdots$		$\vdots$	$\ddots$	
x_l	x_{l-1}	x_{l-2}	$\cdots$	x_{l-r}	$\cdots$	x_1
x_{l+1}	x_l	x_{l-1}	$\cdots$	x_{l-r+1}	$\cdots$	x_2
x_{l+2}	x_{l+1}	x_l	$\cdots$	x_{l-r+2}	$\cdots$	x_3
$\vdots$	$\vdots$	$\vdots$		$\vdots$		$\vdots$
x_{n-2}	x_{n-3}	x_{n-4}	$\cdots$	x_{n-r-2}	$\cdots$	x_{n-l-2}
x_{n-1}	x_{n-2}	x_{n-3}	$\cdots$	x_{n-r-1}	$\cdots$	x_{n-l-1}
x_n	x_{n-1}	x_{n-2}	$\cdots$	x_{n-r}	$\cdots$	x_{n-l}

between the column X_t, and each column X_{t-r}, are examined. In (1), $\bar{x} = (1/n)\sum_{t=1}^{n} x_t$ denotes the sample average of (the column) X_t in Table 1. Note that some sources use an alternative formula that substitutes the term $1/n$, in the numerator of (1), with $1/(n-r)$. Although this definition has less bias, the formulation in (1) has some desirable statistical properties and is the form most commonly used in statistics literature (for details, see Chatfield, 1989, pages 20 and 49–50). In the absence of autocorrelation, the asymptotic distribution of $\widehat{\rho}_r$ in (1), $r = 1,\ldots,l$, is normal; thus, in the autocorrelogram, choosing a significance level α, one can draw upper and lower bounds, for absence of autocorrelation, with limits $\mp z_{1-\alpha/2}/\sqrt{n}$, where $z_{1-\alpha/2}$ is the quantile of the standard normal distribution. In this case, the confidence bands have fixed width that depends on the sample size n.

Logically, through the autocorrelogram, other kinds of specific serial dependences can be considered for investigation transforming the original time series in a convenient way. Thus, for example, if we are interested in evaluating serial linear dependence between squared variables of the process, we can apply the transformation $Y_t = X_t^2$ and compute the ACF on $\{y_1,\ldots,y_n\}$. With this philosophy, McLeod and Li (1983) suggest inserting squared residuals in the Box-Ljung statistic; in doing so the authors solve the problem of checking a possible quadratic correlation but, at the same time, their method may clearly fail to be consistent against different dependence structures. In other words, a clear disadvantage of this approach is its "directional" nature, since it is intended to detect specified alternatives. To solve this problem, in an attempt to provide a more general graphical representation than the autocorrelogram, one could consider rank-based variants of the sample autocorrelation coefficient in (1) as, for example, the well-known indexes of Spearman (1904) and Kendall (1938); for a survey on the use of these coefficients in constructing tests for serial dependence see, for example, Diks (2009). Although the sphere of activity is extended so to investigate more general monotonic serial dependences, the initial problem is still not covered. In fact, it is not hard to construct examples of processes for which statistics of linear and monotonic serial dependence may clearly fail to highlight the real but unknown underlying dependence structure. For instance, the bilinear process

$$X_t = \vartheta X_{t-2}\varepsilon_{t-1} + \varepsilon_t, \quad |\vartheta| < 1,$$

where $\{\varepsilon_t\}$ is a sequence of independent standard normal variables, clearly exhibits a complex form of dependence, but it has neither linear nor monotonic serial dependence structure of any order beyond lag zero.

3 The autodependogram

In this section, motivated by the above considerations, a graphical device is provided designed to detect dependences as a function of the time lags. We recall that the term "dependences" is referred to dependence in a wider sense (distributive dependence). In these terms, the proposal could be defined as "omnibus". Naturally, being omnibus, it will be less powerful than the autocorrelogram when the structure of dependence characterizing the observed time series is the linear one, and less powerful of a representation using rank correlation statistics when the underlying dependence is monotonic.

The proposal draws on Bagnato and Punzo (2010) and considers the problem of studying the generic dependence of lag r by using the well-known and general χ^2-statistic of independence. To address this, the first step consists in creating the bivariate joint distribution in Table 2 of the variables X_t and X_{t-r}, considering the elements highlighted in Table 1. Here, k is the number of classes, supposed to be the same for each variable and for each lag r, and $a_1^{(r)}, \ldots, a_{k-1}^{(r)}$, $a = c, d$, are cutoff points. Naturally, the procedure can be generalized by setting k as a function of r. Thus, the simple χ^2-test can be used to evaluate the dependence of lag r. In particular we denote

$$T_r = \sum_{i=1}^{k} \sum_{j=1}^{k} \frac{\left[n_{ij}^{(r)} - \hat{n}_{ij}^{(r)}\right]^2}{\hat{n}_{ij}^{(r)}}, \tag{2}$$

Table 2: *Two-way contingency table related to the dependence of lag r.*

X_t \ X_{t-r}	$\leq d_1^{(r)}$	$\cdots$	$d_{j-1}^{(r)} \dashv d_j^{(r)}$	$\cdots$	$> d_{k-1}^{(r)}$	
$\leq c_1^{(r)}$	$n_{11}^{(r)}$	$\cdots$	$n_{1j}^{(r)}$	$\cdots$	$n_{1k}^{(r)}$	
$\vdots$	$\vdots$		$\vdots$		$\vdots$	
$c_{i-1}^{(r)} \dashv c_i^{(r)}$	$n_{i1}^{(r)}$	$\cdots$	$n_{ij}^{(r)}$	$\cdots$	$n_{ik}^{(r)}$	
$\vdots$	$\vdots$		$\vdots$		$\vdots$	
$> c_{k-1}^{(r)}$	$n_{k1}^{(r)}$	$\cdots$	$n_{kj}^{(r)}$	$\cdots$	$n_{kk}^{(r)}$	
						$n^{(r)}$

the test statistic, where $n_{ij}^{(r)}$ are the observed frequencies and $\hat{n}_{ij}^{(r)}$ are the theoretical frequencies under the (null) hypothesis of independence of lag r, with $i, j = 1, \ldots, k$. It is well-known that under this condition, T_r is asymptotically distributed as a χ^2 with $(k-1)^2$ degrees of freedom. From now on, in analogy with the autocorrelogram, the statistic T_r in (2) will be referred as AutoDependence Function (ADF). Note that, all considerations and results described so far can also be easily extended to time series with missing data.

Once chosen k, the cutoff points, and l in Table 1, we can plot the ADF as a function of r. In analogy with the autocorrelogram we define such a diagram as autodependogram. Since k is fixed and equal for each lag on the x-axis, we can also superimpose on the same graph, an upper bound at height $\chi^2_{[(k-1)^2;1-\alpha/2]}$, quantile of a χ^2 distribution with $(k-1)^2$ degrees of freedom.

3.1 Choosing the number of classes and the cutoff points

In order to compute T_r in (2), both the number of classes k and the $k-1$ cutoff points $a_1^{(r)}, a_2^{(r)}, \ldots, a_{k-1}^{(r)}$, $a = c, d$, have to be defined.

We construct Table 2 such that the classes of the marginal distributions have the same frequencies (the so-called equifrequency classes). This choice forces the marginal distributions to be discrete uniforms and, once k is fixed, the internal cutoff points are automatically generated. Thus, k remains the only parameter to be chosen in order to construct Table 2.

In choosing k, the number of observations has to be taken into account. Before proceeding, note that both joint frequencies and classes vary by changing compared variables. In particular, from Table 1, it is possible to note that we have $n^{(r)} = n - r$ available observations in constructing Table 2. In order to make valid the rth χ^2-test, the well-known rule of thumb $\widehat{n}_{ij}^{(r)} \geq 5$, for each $i, j = 1, \ldots, k$, should hold. This means that the number of observations, in comparison of lag r, has to satisfy the inequality $n^{(r)} \geq 5k^2$. Being k equal for each comparison and being l the maximum value of r, the following has to hold

$$k \leq \sqrt{\frac{n^{(l)}}{5}} = s. \tag{3}$$

Equifrequency classes make it easier to guarantee this condition.

In order to select k among its possible values in the set $S = \{2, \ldots, \lfloor s \rfloor\}$, where $\lfloor \cdot \rfloor$ is the floor function, considerations about the power of the l χ^2-tests can be made. In fact, while the significance level α should be preserved at the varying of k, the power can be maximized. To obtain this, in the following we provide a simple method, that instead of using α, takes into account the more general concept of p-value. Other more sophisticated techniques can be considered however.

Let p_{rk} be the p-value of the rth χ^2-test obtained using k classes, $k \in S$ and $r = 1, \ldots, l$. For each $k \in S$, consider the vector $\mathbf{p}_k = (p_{1k}, \ldots, p_{lk})'$. A natural way to maximize the power consists in choosing k such that $\mathbf{p}_k$ contains values as close as possible to zero. Then, a very simple choice for k could be the following:

$$k^* = \underset{k \in S}{\operatorname{argmin}} \left\| \mathbf{p}_k \right\|, \tag{4}$$

where $\|\cdot\|$ denotes the L^2-norm.

4 Illustrative examples and simulations

This section pursues the aim of evaluating the performance of the ADF using simulated data with gradual departure from serial independence. This performance is compared with that of the ACF. Some simple generated series from famous models in the time series literature, are preliminarly considered in order to directly display the behavior of the autodependogram. A comparison with the autocorrelogram will be always provided.

In what follows, the nominal size will be fixed at 0.05 and the value of k in the autodependogram will always be computed according to rule (4). To perform these numerical experiments we use the `R` environment. The `R` code necessary to compute the ADF and to plot the corresponding autodependogram, is available from the authors upon request. Finally note that, according to Tsay (2005), we will plot the autocorrelogram without the traditional noninformation unit spike at lag 0.

4.1 Two simple examples

Two series, of length $n = 800$, are respectively generated from a MA(1), and a quadratic MA(1), both with parameter 0.8. A standard Gaussian noise, and a maximum lag $l = 30$, are adopted. Results are displayed in Figure 1. Note that,

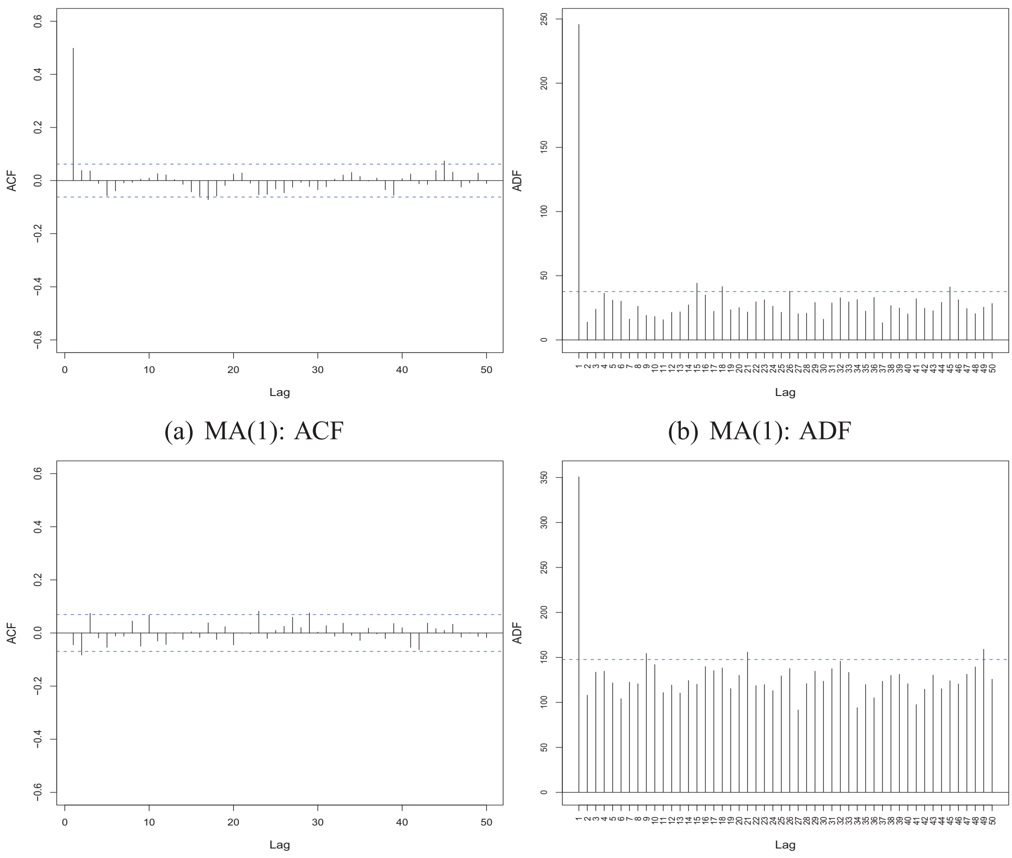

(a) MA(1): ACF

(b) MA(1): ADF

(c) Quadratic MA(1): ACF

(d) Quadratic MA(1): ADF

Figure 1: *Sample ACF, on the left, and sample ADF, on the right, computed on two series generated respectively from a MA(1), and a quadratic MA(1), both with parameter 0.8 ($n = 800$ and $\alpha = 0.05$).*

as said before, the horizontal dotted line, placed at height $\chi^2_{\left[(k-1)^2;0.975\right]}$, makes it easy to identify lags for which the null hypothesis of independence does not hold at the nominal level 0.05.

The examples results can be summarized as follows: in the linear case, for the MA(1), ADF and ACF provide similar information; a significant spike at the first lag, and bars that are almost all included in the confidence bands for the other lags. These are respectively displayed both in Figure 1(b) and Figure 1(a).

Such concordant behavior has also been observed for series (whose results are not here reported) generated from other linear models of the more general ARMA class. In the nonlinear case for the quadratic MA(1), only the autodependogram highlights dependence: in Figure 1(d), in fact, there is a spike at lag 1 and almost no dependence for the other lags. Note that, differently from the autocorrelogram which gives an indication of the percentage of the maximum (linear) dependence, the ADF, by construction, can not measure the relative impact of dependence for the generic lag. Nevertheless, each bar of the ADF can be compared with the other ones; for example, ADF in Figure 1(d) highlights that dependences of lags greater than 2 are less intense than the dependence of lag 1.

4.2 Simulations

In this section, three sets of Monte Carlo experiments are shown in order to compare the performance of the autocorrelogram and the autodependogram considering a maximum lag $l = 30$. A wide scenario of situations is considered including independence, linear and nonlinear dependence. The subsets of models used in each scenario are specified in the third column of Table 3. For the indepen-

Table 3: *Adopted models.*

Context	Model	Specification
Independence	(A) Cauchy	u_t
	(B) Bimodal Gaussian Mixture	υ_t
Linear dependence	(C) MA(q)	$X_t = \sum_{j=1}^{q} \vartheta_j \varepsilon_{t-j} + \varepsilon_t$
	(D) AR(p)	$X_t = \sum_{j=1}^{p} \vartheta_j X_{t-j} + \varepsilon_t$
Noninear dependence	(E) ARCH(p)	$X_t = \sigma_t \varepsilon_t, \quad \sigma_t^2 = 1.5 + \sum_{j=1}^{p} \vartheta_j X_{t-j}^2$
	(F) GARCH(1,1)	$X_t = \sigma_t \varepsilon_t, \quad \sigma_t^2 = 1.5 + \vartheta_1 X_{t-1}^2 + \eta_1 \sigma_{t-1}^2$
	(G) Quadratic MA(q)	$X_t = \sum_{j=1}^{q} \vartheta_j \varepsilon_{t-j}^2 + \varepsilon_t$
	(H) Bilinear AR(2)	$X_t = \vartheta_1 X_{t-2} \varepsilon_{t-1} + \varepsilon_t$

dence case, noise is generated from a standard Cauchy (denoted with u_t) and from a bimodal normal mixture[1] (denoted with v_t), while a standard normal (denoted with ε_t) is always used under linearity and nonlinearity. The parameters for models in Table 3 are chosen in order to guarantee stationarity. With the exception of the serial independence case, two different sets of parameters are considered for each model in order to fully appreciate the dynamic of the estimated power. For each model, 1000 samples are generated. For each of them, a time series of length 900 is generated, with only the final $n = 800$ observations used. Rejection rates, of both ACF and ADF, are so recorded for each lag r, $r = 1, \dots, l$ (here, the rth rejection rate has to be understood to mean the percentage of times that the rth bar exceeds the confidence bands). We recall that the value of k in each repetition is selected according to (4). To facilitate size evaluation in all displayed plots, a dotted horizontal line is placed at height 0.05.

Figure 2 shows results in the context of independence. The ADF for both of the

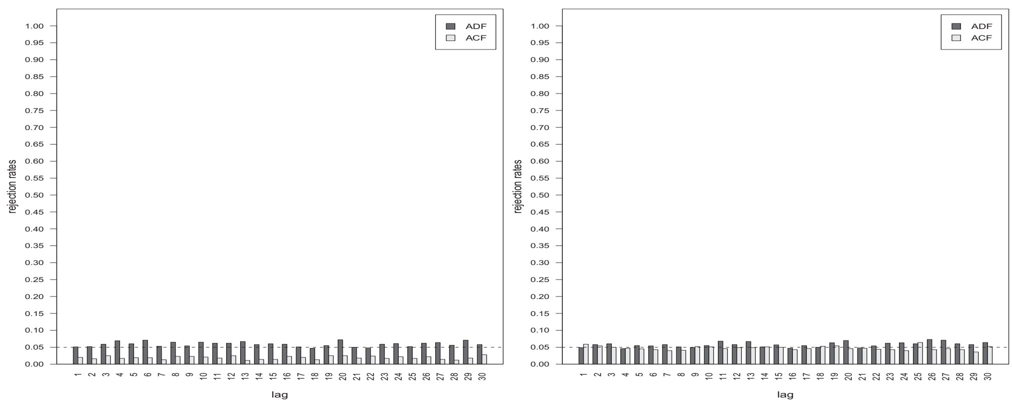

(a) Cauchy (b) Bimodal normal-mixture

Figure 2: *Rejection rates of ACF and ADF computed on* 1000 *series, of length* $n =$ 800*, arising from model (A), on the left, and model (B), on the right, of Table 3.*

simulated noises shows an empirical size close to the nominal one for each of the 30 considered lags. On the other hand, the ACF behaves according to expectations when the noise is generated from the bimodal normal mixture (see Figure 2(a)), but it tends to be more conservative in the other case (see Figure 2(b)).

Figure 3 displays results in the context of serial linear dependence. Here, the set of parameters are chosen in order to highlight the best performance of the autocorrelogram. However, further simulation results (not reported here) show that the disparity in terms of estimated power between the two dependence functions, decreases when the degree of linear dependence increases. For example,

[1] The density is $6/10\phi(x; -5/3, 1) + 4/10\phi(x; 5/2, 1)$, where $\phi(\cdot; \mu, \sigma)$ denotes a normal density with mean μ and standard deviation σ. It ensures: zero mean, bimodality and skewness.

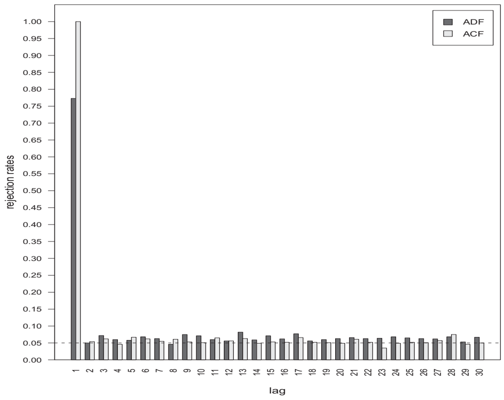

(a) MA(1):$\vartheta_1 = 0.2$

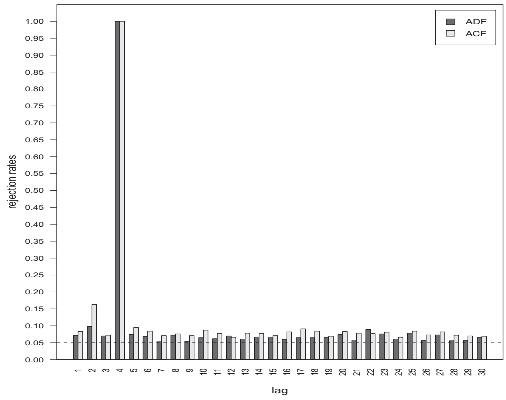

(b) MA(4):$(\vartheta_1, \vartheta_2, \vartheta_3, \vartheta_4) = (0, 0, 0, 0.4)$

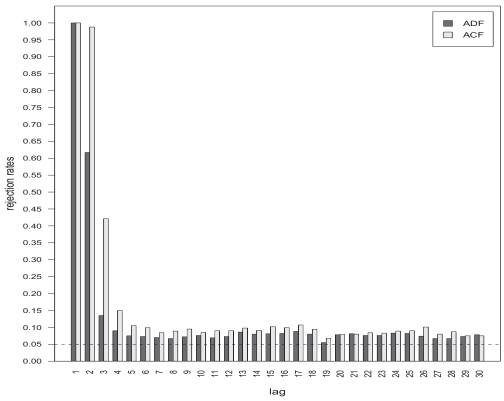

(c) AR(1): $\vartheta_1 = 0.4$

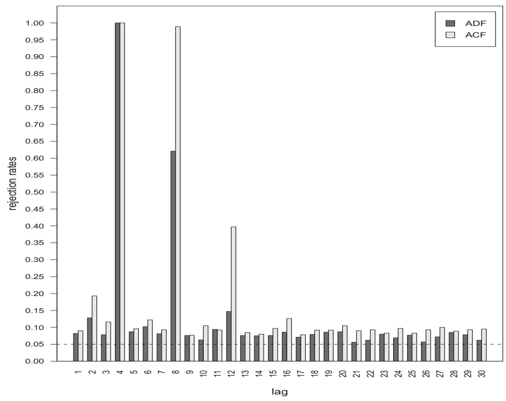

(d) AR(4): $(\vartheta_1, \vartheta_2, \vartheta_3, \vartheta_4) = (0, 0, 0, 0.4)$

Figure 3: *Rejection rates of ACF and ADF computed on* 1000 *series, of length* $n = 800$*, arising from model (C) and model (D) of Table 3.*

as regards the MA(1), ADF and ACF already behave practically in the same way when $\vartheta_1 = 0.3$. Generally, regardless of the chosen parameters, the two graphical devices are characterized by the same underlying structure for all diagrams in Figure 3.

Finally, in Figure 4 the rejection rates are jointly represented for two different sets of parameters of the nonlinear models in Table 3. In this case, the results are inverted with respect to the previous one. More specifically, although ACF and ADF show the same general pattern also in this case, the latter seems to be more powerful above all for the quadratic MA model of Figure 4(e) and Figure 4(f). Moreover, since the adopted models have zero-correlation, the estimated power for the ACF should be near the nominal size. This means that the ACF, in these cases, wrongly displays linear dependences; this is probably due to the fact that dependence structure of the series can be approximated, in some way and degree,

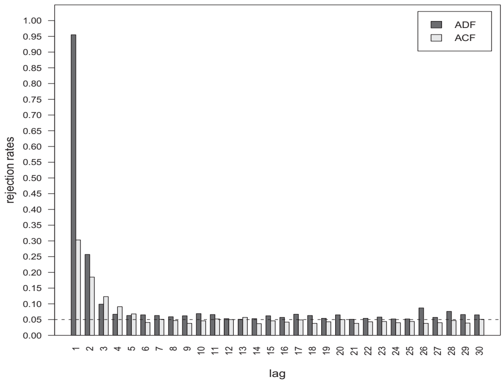

(a) ARCH(1): $\vartheta_1 = 0.6$

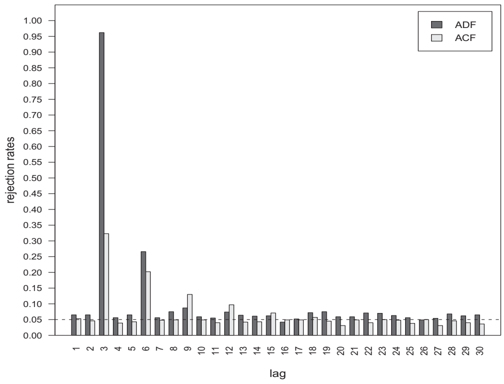

(b) ARCH(3): $(\vartheta_1, \vartheta_2, \vartheta_3) = (0, 0, 0.6)$

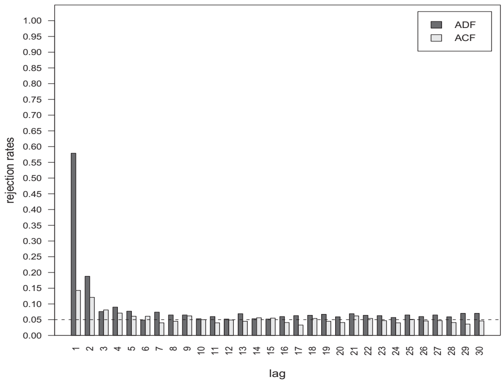

(c) GARCH(1,1): $(\vartheta_1, \eta_1) = (0.3, 0.3)$

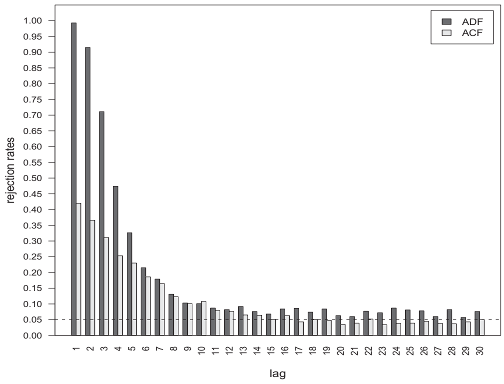

(d) GARCH(1,1): $(\vartheta_1, \eta_1) = (0.6, 0.3)$

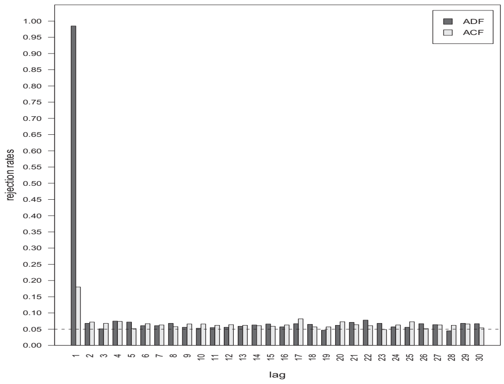

(e) Quadratic MA(1): $\vartheta_1 = 0.8$

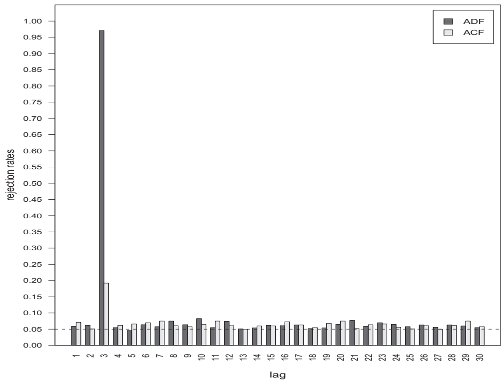

(f) Quadratic MA(3): $(\vartheta_1, \vartheta_2, \vartheta_3) = (0, 0, 0.8)$

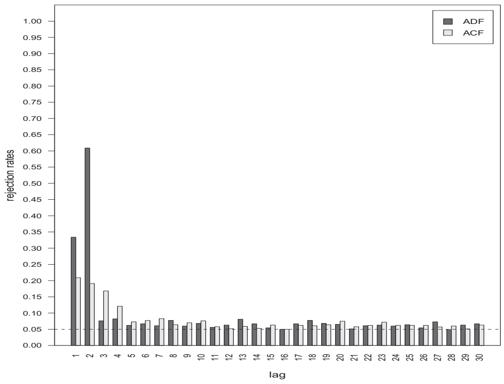

(g) BILINEAR: $\vartheta_1 = 0.6$

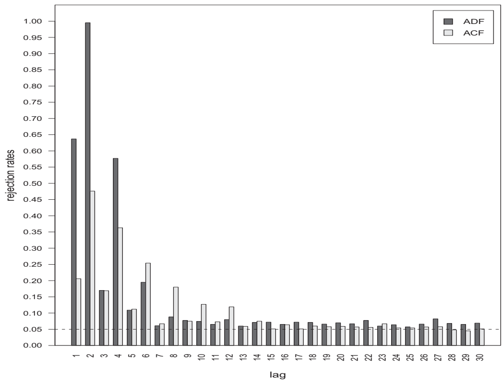

(h) BILINEAR: $\vartheta_1 = 0.9$

Figure 4: *Rejection rates of ACF and ADF computed on* 1000 *series, of length* $n = 800$*, arising from models (E), (F), (G), and (H) of Table 3.*

by the linear one.

5 Real applications

In this Section, in order to show the potential of the autodependogram in detecting nonlinear dependences, we apply the ADF to both an environmental time series (ozone concentrations) and an economic one (natural gas prices). A comparison with the ACF will be also given.

5.1 Ozone concentrations

As first real field of application, we consider the hourly ozone concentrations measured by a single monitoring site, located in via Juvara, Milano (North of Italy), during the period 2002–2006 (see Figure 5). Data have been gathered and their quality assessed, by the Lombardia ARPA (Agenzia Regionale per la Protezione Ambientale, *i.e.* Regional Environmental Protection Agency) and they can be downloaded from the web site
`http://ita.arpalombardia.it/ITA/qaria/doc_RichiestaDati.asp`.

The time series of ozone is typically characterized by nonlinear components arising from the chemical process underlying its formation. Ozone concentrations are produced as a secondary pollutant by a chemical reaction of NOx with volatile organic compounds (VOCs), an important class of air pollutants commonly found in the atmosphere at ground level in all urban and industrial centers.

The photochemical reactions that produce ozone depend on meteorological conditions such as solar radiation, wind speed, temperature and pressure. The influence of these variables makes the ozone series highly seasonal. Wind speed determines transport and accumulation of primary pollutants and temperature directly influences the kinetics of reactions producing ozone and determines the mixing height, which affects the accumulation of primary pollutants. The solar radiation acts directly on the ozone concentrations producing minimum values in winter and maximum values in summer. A daily cycle is also present producing a peak in concentration during the warmer hours of the day and a reduction at night (see Cocchi and Trivisano, 2002; Nicolis and Fassò, 2002). Small seasonal variations depend essentially on the local climatic peculiarities and on the land use. Many models have been proposed in literature for studying the nonlinear behavior of time series in general (see, *e.g.*, the recent work of Chen *et al.*, 2010), and with respect to ozone concentrations (see, *e.g.*, Niu, 1996; Chen *et al.*, 1998; Fassò and Negri, 2002; Nicolis, 2002). In particular, Nicolis (2002) uses wavelet transforms for decomposing the ozone series in different frequency components reflecting the cyclical components of the data.

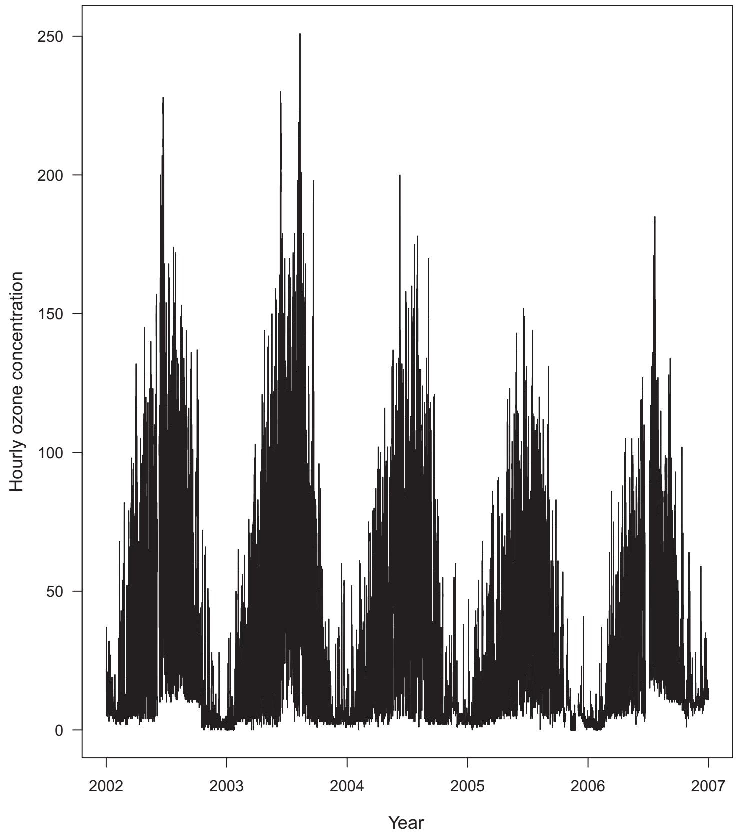

Figure 5: *Hourly ozone concentrations from 1/1/2002 to 31/12/2006.*

This application shows that the autodependogram is a powerful tool for detecting nonlinear components in environmental time series. In particular, the autodependogram of hourly ozone concentrations, in Figure 6(b), highlights not only the dominant daily cyclical component but also the intra-day cycle due to the variation of temperature and solar radiation. In fact, the absence of solar radiation during the night associated with the emission of NOx in the urban areas causes the conversion reaction. This intra-day component is not detected by the standard autocorrelogram where the linear trend is dominant Figure 6(a).

5.2 Natural gas prices

As second real field of application, we consider the economic one. In particular, in recent years the electric power industry has undergone many fundamental and unprecedented changes due to the process of deregulation. Time series of prices in this sector are often characterized by multi-scale seasonality, high volatility and spiking behavior. An increasing amount of works has tried to describe the ex-

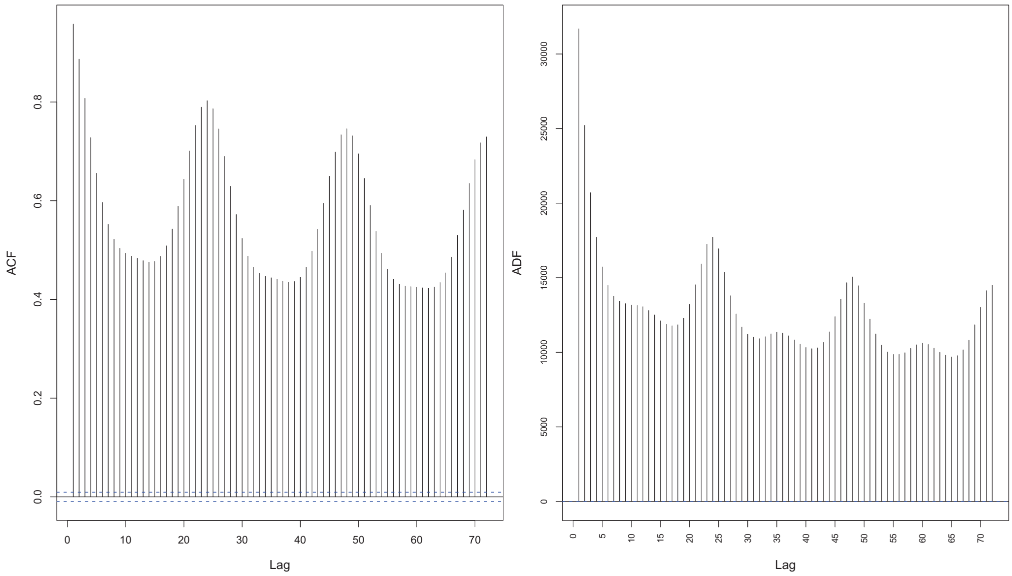

(a) ACF (b) ADF

Figure 6: *ACF and ADF of hourly ozone concentrations.*

post properties of the market prices and to specify adequate econometric models to describe the delicate, nonlinear and evolutionary interactions of fundamental and market conduct variables known to influence power price formation (see, *e.g.*, Robinson 2000, Bunn 2000, Benaouda *et al.* 2006, Weron 2006, and Chen *et al.* 2010).

In this example we consider monthly data for US Natural Gas Industrial Prices (Dollars per Thousand Cubic Feet), freely available from the web page

`http://www.eia.gov/dnav/ng/ng_pri_sum_dcu_nus_m.htm`,

for the period ranging from October 1983 to August 2010 (Figure 7).

Figure 8 shows the ACF and ADF plots of monthly series of natural gas prices. While the ACF shows a strong linear trend that occurred in the last ten years, the ADF detects nonlinear dependences at different lags. For example, the ADF shows an evident peak around the lag 36 (three years), and other small but prominent humps for the subsequent lags; among them it is possible to note a peak around lag 84 (seven years). These dependences are shown by ACF only on the detrended series, that is, after applying a first order differentiation (see Figure 9). This example wants to highlight that while the ADF is able to detect all the dependences, the ACF needs a preliminary transformation of the series, especially when the trend component is strong. Moreover, using ACF many problems arises when we do not know the transformation to use.

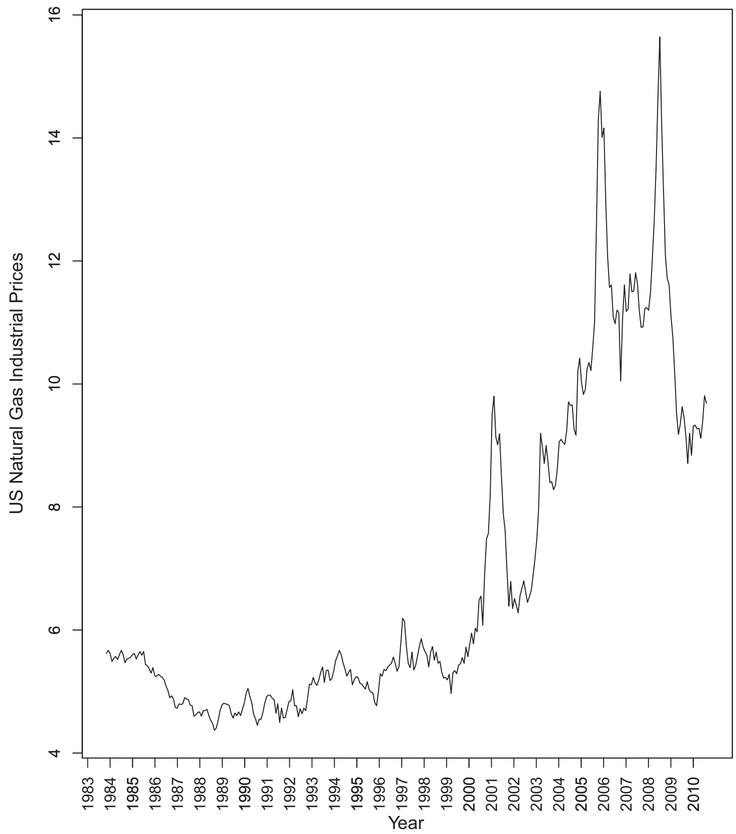

Figure 7: *US Natural Gas Industrial Prices (Dollars per Thousand Cubic Feet) from October 1983 to August 2010.*

6 Conclusions and discussion

In this paper, we present a new graphical device that we have chosen to call autopependogram, with the aim of graphically investigating (serial) dependences as a function of the time lags. The proposal takes advantage of the simple setting characterizing the famous autocorrelogram and exploits the simple and well-known χ^2-statistic of independence. Such a choice allows us to easily detect dependences that are more general than, for example, the linear or monotonic ones. Applications and simulations show the good performance of the autodependogram in situations where the autocorrelogram is applicable too highlighting its usefulness when the time series is nonlinear.

Further effort can be devoted to solve one criticism of the ADF T_r: it, in fact, does not give a meaningful description of the degree of dependence for lag r. In other words, it is useful for determining whether there is dependence but it is not easy to interpret the strength of that dependence. Thus, it could be useful

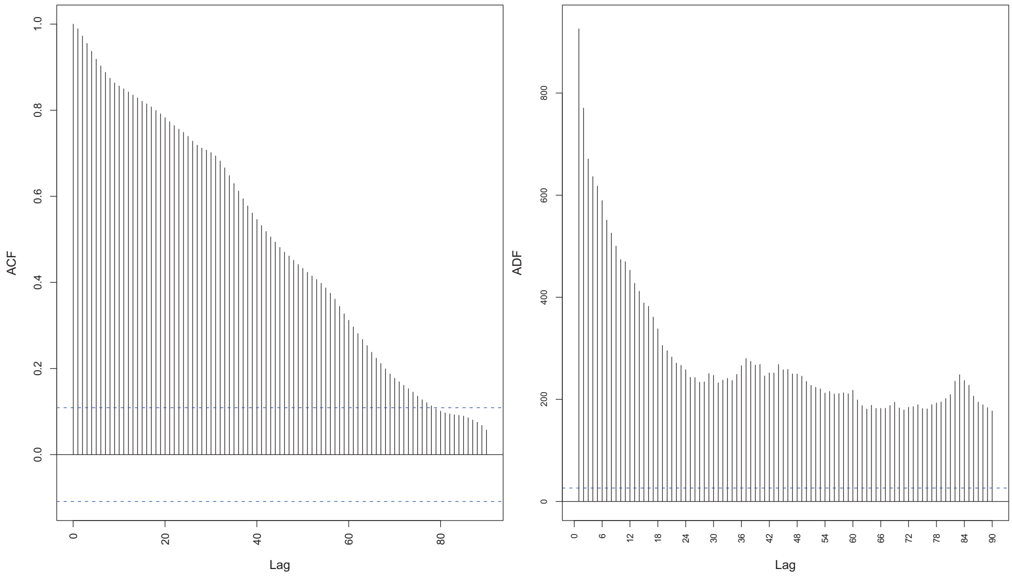

(a) ACF (b) ADF

Figure 8: *ACF and ADF of Monthly Natural Gas Prices.*

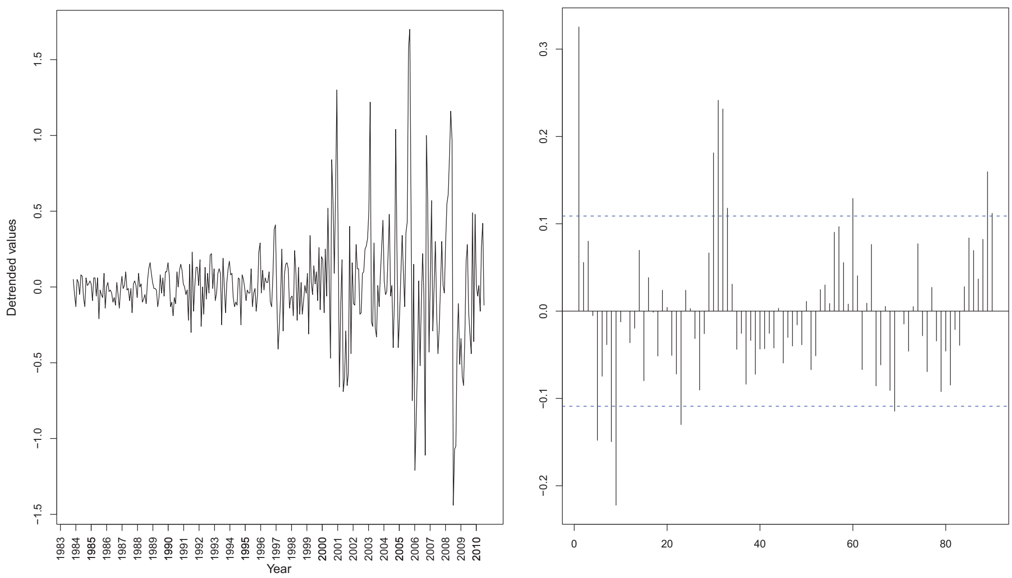

(a) Detrended series (b) ACF

Figure 9: *Detrended series of Monthly Natural Gas Prices and its ACF.*

to provide a normalized statistic, taking values in the compact interval $[0, 1]$. In these terms, Cramer's contingency coefficient would provide an easier to interpret measure of strength of dependence. With our notation, it is defined as

$$C_r = \sqrt{\frac{T_r}{n(k-1)}}, \tag{5}$$

monotone transformation of T_r. This statistic is based on the fact that the maximum value of T_r is $n(k-1)$. So, C_r basically scales T_r to a value between 0 (no dependence) and 1 (maximum dependence). It has the desirable property of scale invariance, that is, if the sample size n increases, the value of Cramer's contingency coefficient in (5) does not change as long as values in the table change the same relative to each other. Moreover, the C_r statistic, like the ACF, is dimensionless, that is, independent of the scale of measurement of the time series. Finally, it is interesting to note, that applying the same transformation in (5) to the critical value $\chi^2_{[(k-1)^2;1-\alpha/2]}$, one obtains a sort of "normalized" upper bound that can be superimposed on the diagram of the normalized ADF in order to evaluate randomness of the observed time series. Nevertheless, we do not use Cramer's index because it has a substantial defect. In fact, as well-known, it attains values near to its maximum very sporadically. This consideration motivates the search for other normalized indexes not affected by this inconvenient.

Acknowledgements

The authors sincerely thank the Professor Domenico Piccolo for his very helpful comments and suggestions.

References

Bagnato, L. and Punzo, A. (2010). On the Use of χ^2-Test to Check Serial Independence. *Statistica & Applicazioni*, **VIII**(1), 57–74.

Benaouda, D., Murtagh, F., Starck, J., and Renaud, O. (2006). Wavelet-based nonlinear multiscale decomposition model for electricity load forecasting. *Neurocomputing*, **70**(1–3), 139–154.

Bera, A. and Robinson, P. M. (1989). Tests for Serial Dependence and Other Specification Analysis in Models of Markets in Disequilibrium. *Journal of Business & Economic Statistics*, **7**(3), 343–352.

Booth Teppo, G. and Yli-Olli, P. (1994). Nonlinear dependence in Finnish stock returns. *European Journal of Operational Research*, **74**(2), 273–283.

Brock, W., Dechert, W., Scheinkman, J., and LeBaron, B. (1996). A test for independence based on the correlation dimension. *Econometric Reviews*, **15**(3), 197–235.

Bunn, D. (2000). Forecasting loads and prices in competitive power markets. *Proceedings of the Institute of Electrical and Electronics Engineers*, **88**(2), 163–169.

Chatfield, C. (1989). *The Analysis of Time Series: An Introduction*. Chapman & Hall, New York, fourth edition.

Chen, H., Nicolis, O., and Vidakovic, B. (2010). Multiscale forecasting method using ARMAX models. *Current Development in Theory and Applications of Wavelets*, **...**(...), ...–...

Chen, J., Islam, S., and Biswas, P. (1998). Nonlinear dynamics of hourly ozone concentrations nonparametric short term prediction. *Atmospheric environment*, **32**(11), 1839–1848.

Cocchi, D. and Trivisano, C. (2002). Ozone. In A. El-Shaarawi and W. Piegorsch, editors, *Encyclopedia of Environmetrics*, pages 1518–1523. Wiley, New York.

Diks, C. (2009). Nonparametric tests for independence. In R. A. Meyers, editor, *Encyclopedia of Complexity and Systems Science*, pages 6252–6271. Springer, New York.

Diks, C. and Panchenko, V. (2007). Nonparametric tests for serial independence based on quadratic forms. *Statistica Sinica*, **17**, 81–98.

Dufour, J., Lepage, Y., and Zeidan, H. (1982). Nonparametric testing for time series: a bibliography. *Canadian Journal of Statistics*, **10**(1), 1–38.

Fassò, A. and Negri, I. (2002). Nonlinear statistical modelling of high frequency ground ozone data. *Environmetrics*, **13**(3), 225–241.

Genest, C. and Rémillard, B. (2004). Test of independence and randomness based on the empirical copula process. *Test*, **13**(2), 335–369.

Hallin, M. and Puri, M. (1992). Rank tests for time series analysis: a survey. In D. Brillinger, E. Parzen, and M. Rosenblatt, editors, *New Directions in Time Series Analysis*, pages 111–153, New York. Springer-Verlag.

Jianqing, F. and Qiwei, Y. (2003). *Nonlinear time series: nonparametric and parametric methods*. Springer.

Kendall, M. (1938). A new measure of rank correlation. *Biometrika*, **30**(1–2), 81.

Lo, A. W. (2000). Finance: A selective survey. *Journal of the American Statistical Association*, **95**(450), 629–635.

McLeod, A. and Li, W. (1983). Diagnostic checking ARMA time series models using squared-residual autocorrelations. *Journal of Time Series Analysis*, **4**(4), 269–273.

Moran, P. (1953). The statistical analysis of the Canadian lynx cycle, i: Structure and prediction. *Australian Journal of Zoology*, **1**, 163–173.

Nicolis, O. (2002). Wavelets e reti neurali: analisi e previsione dell'ozono. In R. Colombi and A. Fassò, editors, *Statistical Monitoring for Enviromental Engineering: Models and Applications to Bergamo Country*. Bergamo University Press, Edizioni Sestante, Bergamo, Italy.

Nicolis, O. and Fassò, A. (2002). Air quality in Bergamo area: a statistical descriptive analysis of the last decade. In R. Colombi and A. Fassò, editors, *Statistical Monitoring for Enviromental Engineering: Models and Applications to Bergamo Country*. Bergamo University Press, Edizioni Sestante, Bergamo, Italy.

Niu, X. (1996). Nonlinear Additive Models for Environmental Time Series, with Applications to Ground-Level Ozone Data Analysis. *Journal of the American Statistical Association*, **91**(435), 1310–1321.

Robinson, T. (2000). Electricity pool prices: a case study in nonlinear time-series modelling. *Applied Economics*, **32**(5), 527–532.

Spearman, C. (1904). The Proof and Measurement of Association between Two Things. *The American Journal of Psychology*, **15**(1), 72–101.

Tjøstheim, D. (1994). Non-linear time series: A selective review. *Scandinavian Journal of Statistics*, **21**, 97–130.

Tsay, R. S. (2005). *Analysis of financial time series*. John Wiley & Sons, New Jersey, second edition.

Weron, R. (2006). *Modelling and forecasting electricity loads and prices: a statistical approach, 2006*. John Wiley & Sons.